Ultrastructural Pathology

ISSN: 0191-3123 (Print) 1521-0758 (Online) Journal homepage: www.tandfonline.com/journals/iusp20

Not Only Melatonin but also Caffeic Acid Phenethyl Ester Protects Kidneys against Aging-related Oxidative Damage in Sprague Dawley Rats

Mukaddes Eşrefoğlu Professor, Mustafa Iraz Associate Professor, Burhan Ateş Associate Professor & Mehmet Gül Associate Professor

To cite this article: Mukaddes Eşrefoğlu Professor, Mustafa Iraz Associate Professor, Burhan Ateş Associate Professor & Mehmet Gül Associate Professor (2012) Not Only Melatonin but also Caffeic Acid Phenethyl Ester Protects Kidneys against Aging-related Oxidative Damage in Sprague Dawley Rats, Ultrastructural Pathology, 36:4, 244-251, DOI: 10.3109/01913123.2012.679351

To link to this article: https://doi.org/10.3109/01913123.2012.679351

Published online: 31 Jul 2012.

Ultrastructural Pathology, 36(4), 244–251, 2012

ISSN: 0191-3123 print/1521-0758 online
DOI: 10.3109/01913123.2012.679351

informa
healthcare

ORIGINAL ARTICLE

Not Only Melatonin but also Caffeic Acid Phenethyl Ester Protects Kidneys against Aging-related Oxidative Damage in Sprague Dawley Rats

Mukaddes Eşrefoğlu, Professor[1], Mustafa Iraz, Associate Professor[2], Burhan Ateş, Associate Professor[3], and Mehmet Gül, Associate Professor[4]

[1]Department of Histology and Embryology, Faculty of Medicine, Bezmialem Vakif University, Istanbul, Turkey, [2]Department of Pharmacology, Faculty of Medicine, Bezmialem Vakif University, Istanbul, Turkey, [3]Department of Chemistry, Faculty of Science and Art, Inonu University, Malatya, Turkey, and [4]Department of Histology and Embryology, Faculty of Medicine, Inonu University, Malatya, Turkey

ABSTRACT

Microscopic features and antioxidant status of kidneys of young, old, and caffeic acid phenethyl ester (CAPE) and melatonin administered old Sprague Dawley rats were evaluated. Aging-related tubular and glomerular changes were evident. The most prominent tubular alterations were massive vacuole formation, mitochondrial degeneration, and lysosome accumulation. Mean tissue malondialdehyde (MDA) level was increased, mean tissue superoxide dismutase (SOD), catalase (CAT) ($p < .001$), and glutathione peroxidase (GPx) activities ($p < .05$), and total glutathione (GSH) level were decreased in old animals. Melatonin significantly reduced tissue MDA levels ($p < .005$), but increased tissue SOD ($p < .001$), CAT, and GPx activities ($p < .05$), and GSH levels ($p < .005$) in old animals. CAPE also significantly reduced tissue MDA levels ($p < .005$), but increased tissue SOD ($p < .05$), CAT ($p < .005$), GPx activities, and GSH levels ($p < .001$) in old rats. Mean tissue MDA levels of melatonin and CAPE-administered rats were even lower than those of young rats ($p < .05$). In conclusion, tubular and glomerular structures and tissue antioxidant enzyme activities were very well preserved in CAPE and melatonin-administered rats.

KEYWORDS: Aging, caffeic acid phenethyl ester, kidney, melatonin, oxidative stress

The oxidative stress theory of aging has become the prominent theory to explain aging at the molecular level. A large amount of research has reported a correlation between increased oxidative damage and age and, a correlation between increased manipulations that increase lifespan and a reduction in oxidative damage and/or increase in resistance to oxidative stress [1]. Free radicals and reactive oxygen species (ROS) in particular play an important part in aging-induced oxidative stress. These are by-products of cell metabolism; particularly in the mitochondria, the lysosomes and the peroxisomes. In general, the majority of ROS are released as by-products of respiration from an electron transport chain located on the mitochondrial inner membrane. Due to the close proximity of ROS generation site and to the high membrane surface, mitochondria become the first potential targets of ROS attack. ROS result in damage to cellular protein, lipids, proteins, and DNA throughout the cell. This damage has been implicated as a cause of aging.

The effects of normal aging on the kidney are both structural and functional. Morphologic changes involve the renal blood vessels, glomeruli, tubules, and interstitium [2]. Renal changes that occur with aging are decrease of renal weight, thickening of the intrarenal vascular intima, sclerogenous changes of the glomeruli, infiltration of chronic inflammatory cells, and fibrosis in the stroma. Altered renal tubular function, including impaired handling of water, sodium, acid, and glucose, is also frequently present in old age [2,3]. Regardless of the anatomic structure initially affected, most chronic renal conditions evolve with destruction of the entire nephron. It is not clear whether the observed decrease in renal function associated with aging is the result

Received 02 November 2011; revised 23 February 2012; accepted 09 March 2012

Correspondence: Prof. Dr. Mukaddes Eşrefoğlu, Bezmialem Vakif University, Tıp Fakultesi, Histoloji ve Embriyoloji AbD, Adnan Menderes Bulvari, Vatan Cad, 34093, Fatih, Istanbul, Turkey. E-mail: drmukaddes@hotmail.com

of intervening pathologic processes, e.g., ischemia (vascular obliteration) or infection, or is the result of a more insidious involutional process [4].

In mammals, including humans, melatonin is produced by and secreted from the pineal gland during the night; however, the nighttime production of melatonin falls markedly with aging such that in senescent animals a nighttime melatonin rise is barely measurable [5, 6]. Melatonin is a highly efficient free radical scavenger and antioxidant both in vitro and in vivo. Furthermore, melatonin greatly potentates the efficiency of previously discovered endogenous and exogenous antioxidants [6]. The loss of this potent antioxidant during aging may be consequential in terms cellular and organismal aging as well the onset of age-related diseases.

Caffeic acid phenethyl ester (CAPE), an active component of propolis produced by honeybees, exhibits antioxidative and anti-inflammatory properties. It has been shown to protect kidneys against carbon tetrachloride [7] and vancomycin toxicity [8] and shock wave-induced renal oxidative damage [9]. To our knowledge; there is no ultrastructural study evaluating the effects of melatonin and CAPE administration on kidney ultrastructure in aging and this is the first experimental study evaluating the effect of CAPE on aging associated kidney damage.

Herein, we aim to investigate light and electron microscopic and biochemical changes in old rats and the effects of melatonin and CAPE administration on these harmful changes.

MATERIALS AND METHODS

Animals and Experimental Protocol

Twenty-eight male Sprague Dawley rats weighing 200–450 g were used. Animals were fed standard rat chow and tap water ad libitum. They were maintained on a 12-h light/12-h dark cycle at 21ºC.

Animals were randomly divided into 4 groups. The first group included 4-month-old rats (young group, $n = 7$), and groups 2–4 included 18-month-old rats (old groups, $n = 7$ each). The animals from group 3 received 5 mg/bw/day melatonin (Old + Mel), and group 4 rats received 15 mg/bw/day CAPE (Old + CAPE), both intraperitoneally for 95 days. Melatonin was dissolved in absolute ethanol and further dilutions were made in saline, with 1% final concentrations of ethanol. CAPE was prepared in the biochemistry laboratory according to standard method described by Grunberg et al. [10]. Animals from groups 1 and 2 were injected with equivalent doses of saline. At the end of the experiment animals were sacrificed by decapitation.

Animal experiments were performed in accordance with the guidelines for animal research from the National Institute of Health and were approved by the Committee of Animal Research at Inonu University, Malatya, Turkey.

Microscopic Examination

Kidneys were rapidly removed and divided to three portions. The first portions were placed in 10% buffered formalin and prepared for routine paraffin embedding. Sections of tissues were cut at 5 µm, mounted on slides, stained with hematoxylin–eosin (HE), Masson's trichrome, and periodic acid–Schiff (PAS). Sections were examined by a Leica DFC280 light microscope and Leica Q Win and Image Analysis system (Leica Micros Imaging Solutions, Cambridge, UK) by a blind observer. Kidney damage was scored by grading glomerular, tubular, and interstitial changes with a maximum score of 21. Glomerular damage (sclerotic changes such as matrix expansion, narrowing or disappearance of the Bowman's space, adhesion of capillary tuft to the Bowman's capsule, capillary collapse, and thickening of glomerular basement membrane) was evaluated as 0, absent; 1, <25% of glomeruli affected; 2, 25–50% of glomeruli affected; 3, >50% of glomeruli affected. Tubular injury was defined as tubular dilatation and tubular atrophy, epithelial degeneration, vacuolization, and tubular cast formation including thyroidization. Grading for each of these tubular changes was scaled as 0, absent; 1, <25% of tubules affected; 2, 25–50% of tubules affected; 3, >50% of tubules affected. The presence of interstitial cell infiltration and congestion were each judged as 0, absent; 1, mild; 2, moderate; 3, severe.

The second part of the tissues was processed for electron microscopic examination. For that purpose, samples were fixed in 2.5% gluteraldehyde buffered with 0.2 M NaH_2PO_4 + $NaHPO_4$ (pH = 7.2–7.3) and postfixed in 1% OsO_4. After dehydration in acetone, they were embedded in Araldite CY 212. Ultrathin sections stained with uranyl acetate and lead citrate were examined in a Carl Zeiss Libra 120 electron microscope.

Biochemical Assays for Determination Oxidative Stress

The rest of the tissue samples were stored at –80°C for the determination of malondialdehyde (MDA), superoxide dismutase (SOD), catalase (CAT), glutathione peroxidase (GSH-Px), and total glutathione (GSH).

Homogenization

Tissues were homogenized (PCV Kinematica Status Homogenizator) in ice-cold phosphate-buffered saline (pH 7.4). The homogenate was sonified with an ultrasonifier (Bronson sonifier 450) for 3 cycles (20-s sonications and 40-s pause on ice). The homogenate was centrifuged (15,000*g*, 10 min, 4°C) and cell-free supernatant was subjected to enzyme assay immediately.

Determination of Enzyme Activities

CAT assay. CAT activity was measured at 37°C by following the rate of disappearance of hydrogen peroxide

(H_2O_2) at 240 nm (ε_{240} = 40 M^{-1} cm^{-1}) [11]. One unit of catalase activity is defined as the amount of enzyme catalyzing the degradation of 1 µmol of H_2O_2 per min at 37°C and specific activity corresponding to transformation of substrate (in µmol) (H_2O_2) per min per mg protein.

SOD assay. SOD (Cu, Zn-SOD) activity in the supernatant fraction was measured using xanthine oxidase/cytochrome c method [12], where 1 unit (U) of activity is the amount of enzyme needed to cause half-maximal inhibition of cytochrome c reduction. The amount of SOD in the extract was determined as units of enzyme mg^{-1} protein, utilizing a commercial SOD as the standard.

GSH-Px assay. GSH-Px activity was determined in a coupled assay with glutathione reductase by measuring the rate of NADPH oxidation at 340 nm using H_2O_2 as the substrate [13]. The enzyme reaction contained 30 mM potassium phosphate, pH 7.0, 1 mM EDTA, 0.2 mM NADPH, 2 mM GSH, 1 mM sodium azide, 1 U glutathione reductase, and 0.1 mM H_2O_2. One unit of GSH-Px is defined as the amount of NADPH (µmol) converted to per min per mg protein.

*GSH assay***.**The total glutathione level was performed using the method of Theodorus et al. with some modifications [14]. The reaction mixture contained 50 mM sodium phosphate, 1 mM EDTA, 0.5 mM DTNB, 0.2 mM NADPH, and 0.5 U/mL of glutathione reductase. Homogenate (10 µL) was added to initiate the reaction but was omitted for control. The formation of 5-thio-2-nitrobenzoate (TNB) is followed spectrophotometrically at 412 nm. The amount of GSH in the extract was determined as nmol/mg protein utilizing a commercial GSH as the standard.

*MDA assay to assess lipid peroxidation***.** The analysis of lipid peroxidation was carried out as described by Buege and Aust [15] with a minor modification. The reaction mixture was prepared by adding 250 µL homogenate into 2 mL reaction solution (15% trichloroacetic acid: 0.375% thiobarbituric acid: 0.25 N HCl, 1:1:1, w/v) and heated at 100°C for 15 min. The mixture was cooled to room temperature and centrifuged (10,000*g* for 10 min), and the absorbance of the supernatant was recorded at 532 nm. 1,1,3,3-Tetramethoxypropane was used as MDA standard. MDA results were expressed as nmol mg^{-1} protein in the homogenate.

Determination of protein. Protein levels of the tissue samples were measured by the Bradford method [16]. The absorbance measurement was taken at 595 nm using a UV-VIS spectrophotometer. Bovine serum albumin (BSA) was used as protein standard.

Statistical Evaluation

Statistical analysis was carried out using the SPSS 10.0 statistical program (SPSS Inc., Chicago, IL, USA). All data are expressed as arithmetic means ± SE. The differences between mean histological damage scores and tissue enzyme levels for each group were analyzed by using one-way analysis of variance (ANOVA) and post hoc Duncan tests. Values of $p < .05$ were regarded as significant.

RESULTS

Biochemical Results

Values for tissue MDA and GSH levels and SOD, CAT, and GPx activities are summarized in Table 1. Mean tissue MDA level was increased in old rats in comparison to young rats, although no statistical importance was detected. Mean tissue SOD, CAT ($p < .001$), and GPx activities ($p < .05$), and GSH level were decreased in old animals. Melatonin significantly reduced tissue MDA levels ($p < .005$), but increased tissue SOD ($p < .001$), CAT, and GPx activities ($p < .05$), and GSH levels ($p < .005$) in old animals. CAPE also significantly reduced tissue MDA levels ($p < .005$), but increased tissue SOD ($p < .05$), CAT ($p < .005$), GPx activities, and GSH levels ($p < .001$) in old rats. Mean tissue MDA levels of melatonin and CAPE administered rats were even lower than those of young rats ($p < .05$).

Histological Results

Tables 2 and 3 depict the semiquantitative data of the histopathological changes. Mean damage score of old rats was statistically higher than that of young rats ($p < .001$). Both melatonin and CAPE administration significantly reduced this parameter ($p < .005$, $p < .05$, respectively). Melatonin and CAPE reduced tubular and epithelial degeneration, sclerosis, cell infiltration, and thyroidization. Both agents significantly reduced tubular dilatation ($p < .05$, $p < .005$; respectively) and epithelial degeneration ($p < .001$, $p < .05$; respectively). Melatonin additionally reduced cell infiltration ($p < .01$). Melatonin and CAPE reduced glomerular sclerosis without statistically significant differences with group 2.

TABLE 1 Mean levels of tissue MDA and GSH, mean activity of tissue SOD, CAT, and GPx in kidneys of the animals from all groups

Groups	MDA (nmol/mg pr)	SOD (U/mg pr)	CAT (U/mg pr)	GP_X (U/ mg pr)	GSH (nmol/mg pr)
Group 1 (Young)	0.54 ± 0.03	4.74 ± 0.43	39.6 ± 1.89	3.95 ± 2.58	22.38 ± 1.51
Group 2 (Old)	0.58 ± 0.04	4.29 ± 0.46	26.64 ± 1.47[e]	3.02 ± 0.25[b]	20.29 ± 1.65
Group 3 (Old + Mel)	0.42 ± 0.03[a,b]	8.92 ± 0.83[c]	31.33 ± 1.64	3.82 ± 0.18[d]	27.94 ± 1.54[a]
Group 4 (Old + CAPE)	0.40 ± 0.02[a,b]	6.61 ± 0.64[d]	34.99 ± 1.45[a]	3.62 ± 0.27	30.26 ± 1.50[c]

Note. Data are expressed as means ± SE; $n = 7$.
[a]$p < .005$ vs. group 2, [b]$p < .05$ vs. group 1, [c]$p < .001$ vs. group 2, [d]$p < .05$ vs. group 2, [e]$p < .001$ vs. group 1.

The specimens of young rats revealed normal kidney histology. The most prominent changes observed in old rats were tubular changes such as vacuolization, tubular dilatation, tubular atrophy, tubular epithelial degeneration (mostly flattening), tubular cast formation, and thyroidization (Figure 1A). Glomerular sclerotic changes (matrix expansion, periglomerular and glomerular collagen deposition, narrowing or disappearance of the Bowman's space, adhesion of capillary tuft to the Bowman's capsule (Figure 1B, C), capillary collapse, thickening of basement membrane of the Bowman capsule (Figure 1D) and that of the glomerulus (Figure 1E), vascular congestion, and interstitial mononuclear cell infiltration (Figure 1D) were also evident.

In both melatonin and CAPE administered rats, the histopathological evidence of age-related kidney damage was markedly reduced (Figure 2A). However, mild epithelial degeneration and congestion and mild to moderate sclerotic changes (Figure 2B) were occasionally observed. Sclerotic changes were more prominent in CAPE administered rats than in melatonin administered ones. Mild congestion was present in both groups (Figure 2B). Tubular atrophy, tubular dilatation, and

TABLE 2 Kidney damage scores of the groups

Groups	Scores for kidney damage
Group 1 (Young)	0.28 ± 0.18
Group 2 (Old)	6.85 ± 1.12[a]
Group 3 (Old + Mel)	3.00 ± 0.81[b]
Group 4 (Old + CAPE)	4.14 ± 0.50[c]

Note. Data are expressed as means ± SE; $n = 7$.
[a]$p < .001$ vs. group 1, [b]$p < .005$ vs. group 2, [c]$p < .05$ vs. group 2.

TABLE 3 Histopathological data of the groups

Groups	Tubular dilatation	Epithelial degeneration	Glomerular sclerosis	Cell infiltration	Congestion	Thyroidization
Group 1 (Young)	0.00 ± 0.00	0.00 ± 0.00	0.12 ± 0.14	0.00 ± 0.00	0.14 ± 0.14	0.00 ± 0.00
Group 2 (Old)	0.57 ± 0.20[a]	1.00 ± 0.00[d]	2.42 ± 0.29[d]	0.85 ± 0.34[f]	1.57 ± 0.36[a]	0.57 ± 0.42
Group 3 (Old + Mel)	0.14 ± 0.14[b]	0.42 ± 0.20[e]	1.57 ± 0.42	0.00 ± 0.00[g]	0.71 ± 0.42	0.14 ± 0.14
Group 4 (Old + CAPE)	0.00 ± 0.00[c]	0.57 ± 0.20[b]	2.00 ± 0.30	0.57 ± 0.20	1.00 ± 0.21	0.00 ± 0.00

Note. Data are expressed as means ± SE; $n = 7$.
[a]$p < .005$ vs. group 1, [b]$p < .05$ vs. group 2, [c]$p < .005$ vs. group 2, [d]$p < .001$ vs. group 1, [e]$p < .001$ vs. group 2, [f]$p < .01$ vs. group 1, [g]$p < .01$ vs. group 2.

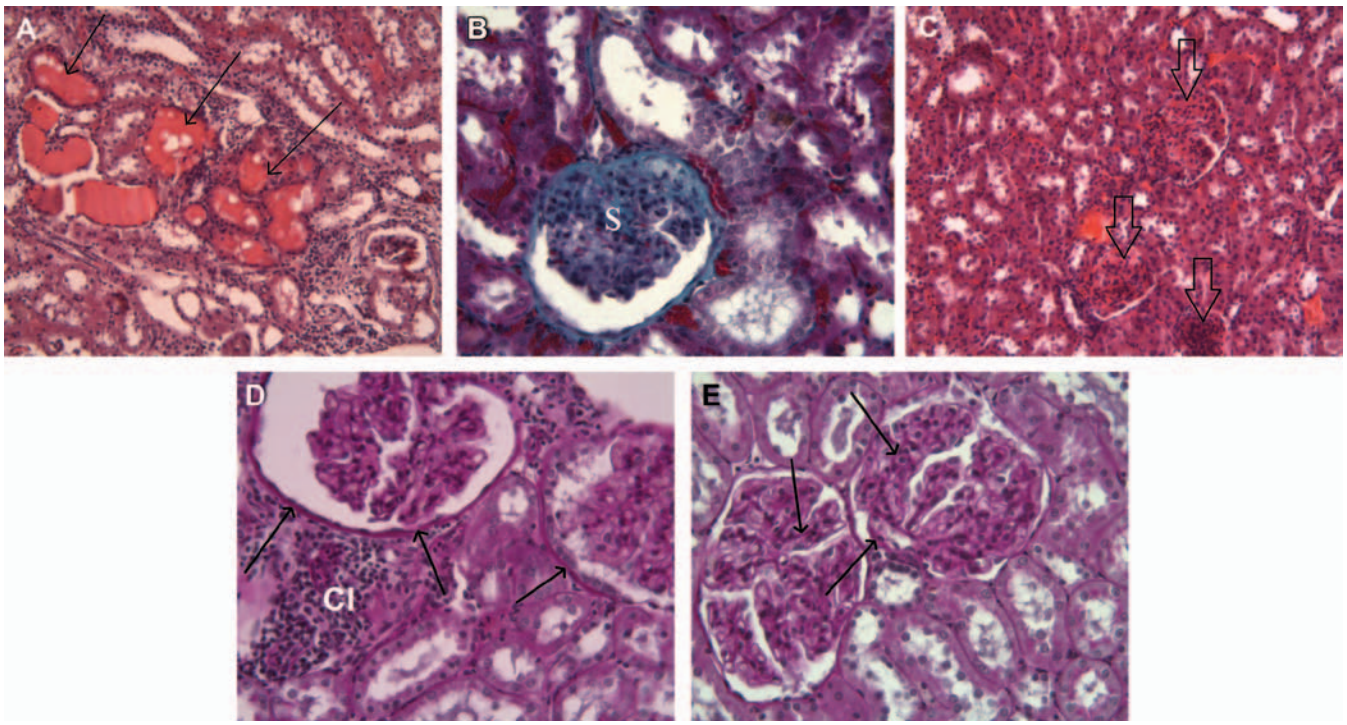

FIGURE 1 Light microscopic images from kidneys of old rats. (A) Tubular epithelial degeneration and thyroidization (arrows) are obvious. Hematoxylin and eosin, ×20. (B) Periglomerular and glomerular collagen deposition and sclerosis (S) are observed. Masson's trichrom method, ×40. (C) Glomerular sclerosis, narrowing, or disappearances of the Bowman's space. The adhesion of capillary tuft to the Bowman's capsule is obvious (arrows). Hematoxylin and eosin, ×20. (D) Thickening of the basal membrane of Bowman's capsule (arrows) and interstitial cell infiltration (CI) are observed. PAS, ×40. (E) Thickening of glomerular basement membranes is seen (arrows). PAS, ×40.

thyroidization were not observed in treated groups. Mononuclear cell infiltration was not observed in melatonin administered rats, whereas mild infiltration was present in CAPE administered ones.

Electron Microscopic Results

By electron microscopy, tubular (Figure 3A, B) and glomerular components (Figure 3C) were normal in young animals. The most prominent aging-induced alterations were edema (Figure 4A), massive vacuole formation, lysosome and lipofuscin accumulation within the tubular cells (Figures 4B, C), and thickening of the tubular basement membranes. Mitochondrial degenerative changes, such as edema, vacuole formation, cristae loss, or thickening of cristae membranes, were observed (Figure 4C). Tubular cells were irregular in shape; microvillus loss and disorganization were obvious. Glomerular basement membranes were also thickened (Figure 4D). Expansion of mesengial matrices was obvious. Some lymphocytes were present in peritubular space. Rarely, tubular cell necrosis was observed. Tubular and glomerular structures were well preserved in CAPE and melatonin administered rats (Figures 5A–C). However, rare vacuole formation and lysosome accumulation were observed (Figure 5D).

DISCUSSION

The natural aging process is associated with progressive structural changes in tissues and organs that eventually result in loss of function followed by tissue/organ failure. Renal structural and functional alterations can lead to the advanced loss of kidney function.

Both tubular and glomerular structures alter during normal aging. Tubular atrophy, with thickening of the basement membrane, is a common feature of parenchymal change, and tubular "thyroidization," with dilatation of the lumen, flattening of tubular epithelium, and accumulation of eosinophilic hyaline cast material within the tubule is also a common feature of end-stage renal tubular damage [4]. We observed all of these alterations in the kidneys of old rats. Tubules were often dilated and filled with pink casts and give an appearance of "thyroidization." There is an increase in the number of glomeruli showing sclerosis with age [3,17,18]. There may be an increase

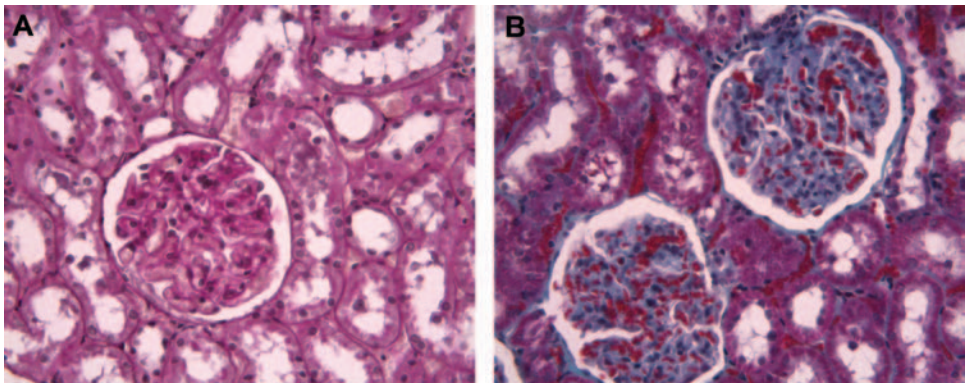

FIGURE 2 Light microscopic images from kidneys of antioxidant-administered old rats. (A) Normal kidney histology of a rat from the Old + CAPE group. PAS, ×40. (B) Mild sclerosis and congestion are observed in the kidney section of a CAPE administered rat. Masson's trichrome method, ×40.

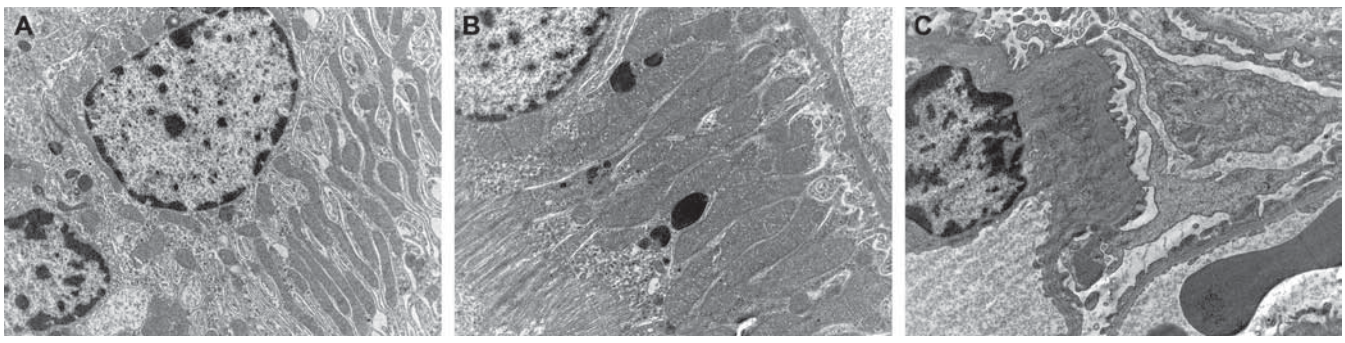

FIGURE 3 Electron microscopic images from kidneys of young rats. (A) A proximal tubule cell containing basal plasma membrane infoldings and many mitochondria is observed. Uranyl acetate and lead citrate, ×8000. (B) A proximal tubule cell containing many microvilli at the apical margin of the cell and many mitochondria throughout cytoplasm. Uranyl acetate and lead citrate, ×8000. (C) Glomerular component is normal in ultrastructural appearance. Uranyl acetate and lead citrate, ×8000.

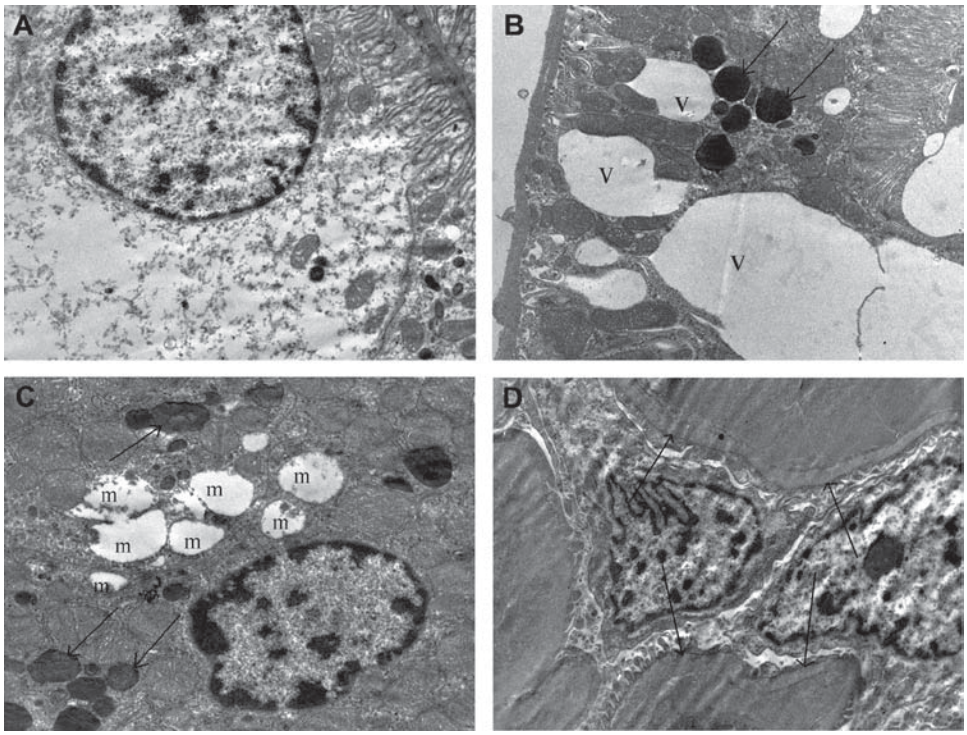

FIGURE 4 Electron microscopic images from kidneys of old rats. (A) Massive edema in a proximal tubule cell is seen. Uranyl acetate and lead citrate, ×10,000. (B) Vacuole formation (V) and lysosome accumulation (arrows) are observed. Uranyl acetate and lead citrate, ×8000. (C) Mitochondrial edema and cristae loss (m) within some of the mitochondria among the healthy ones, and lysosome and lipofuscin accumulation (arrows) are observed. Uranyl acetate and lead citrate, ×10,000. (D) Thickening of glomerular basement membranes (arrows) is seen. Uranyl acetate and lead citrate, ×8000.

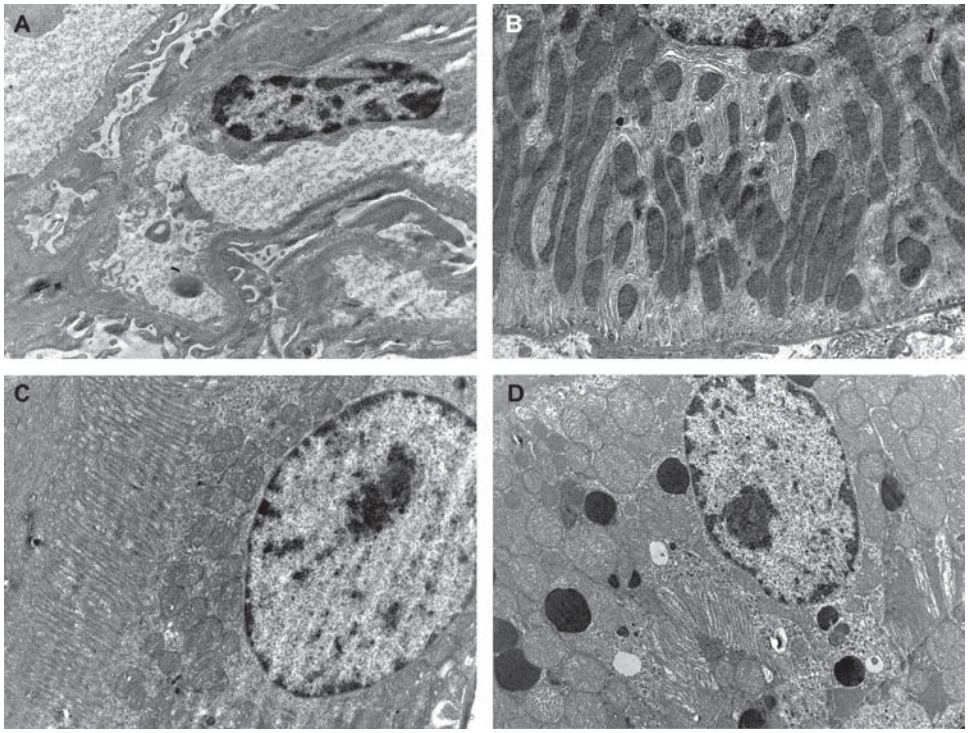

FIGURE 5 Electron microscopic images from kidneys of antioxidant-administered old rats. (A) A kidney section from the Old + CAPE group reveals normal glomerular ultrastructure. Uranyl acetate and lead citrate, ×8000. (B) A kidney section from the Old + Mel group reveals normal tubular ultrastructure. Uranyl acetate and lead citrate, ×8000. (C) A kidney section from the Old + Mel group reveals normal tubular ultrastructure. Uranyl acetate and lead citrate, ×8000. (D) A kidney section from the Old + CAPE group reveals vacuole formation and lysosome accumulation. Uranyl acetate and lead citrate, ×6300.

in the glomerular basement membrane and in the mesengial matrix volume/material [19–21]. These are likely to result from alterations in the balance between formation and breakdown of the extracellular matrix in the glomerulus. Total collagen content increases with age [22]. Another possible explanation for the progressive increase in sclerotic glomeruli with age is glomerular ischemia secondary to the changes in renal blood flow that occur with age [23]. Sclerosis, matrix expansion, and glomerular basement membrane thickening were the most obvious alterations observed in old rats in the present study. The development of progressive glomerulosclerosis occurs in multiple renal diseases as well as in physiological aging [24].

The cellular mechanisms of aging have been the focus of a great deal of study over the last decade. The key findings in relation to aging kidney are subcellular changes, such as brush border abnormalities [25], mitochondrial changes [26] and lipofuscin accumulation [27], DNA mutation abnormalities [28,29], telomere shortening [30,31], and oxidative stress [29]. Since mitochondria are particularly sensitive to oxidant damage, they seem to play a key role in the aging process. Tissues isolated from aging animals usually have several changes in mitochondrial structure, such as swelling, shortening or loss of the cristae, matrix vacuolization, condensation, and myelinic figure formation [33–36]. These changes have been related to an increased generation of superoxide anion and hydrogen peroxide and a decline in the capacity for energy production [35]. We have recently reported cristae loss, vacuolization and myelin figure formation within the mitochondria of cerebral and cerebellar neurons [34] and cardiac myocytes [37] of chronologically aged rats. Our present results support age-related mitochondrial changes in the tubular epithelial cells of old rats. de Cavanagh et al. [36] observed a high number of epithelial cells showing either the absence of microvilli or the presence of altered microvilli in proximal tubules of old rats. We observed microvilli loss and disorganization in old rats. The number of lysosome and lipofuscin granules represents the amount of by-products within the cell. Aged cells have increased numbers of lipofuscin granules.

Much attention has recently been focused on the hypothesis that free radical production may contribute to cellular and organismal aging. Reactive oxygen species enhance aging owing to their ability to attack cellular constituents such as DNA, proteins, and lipids. Increases of some aging markers (e.g., lipid peroxide) have been observed with aging [34, 38]. MDA is a metabolic product of lipid peroxidation. The levels of tissue MDA are often used as a marker of oxidative damage and as an indicator of aging. GPx and SOD are the important antioxidant enzymes in vivo. SOD catalyzes the dismutation of superoxide to oxygen and hydrogen peroxide [12], which is catalyzed next by GPx with GSH as an electron donor [39]. It has been shown that the level of MDA increases, but GPx and SOD activity decreases in kidney with aging [40,41].

Lipid peroxidation brings about several changes in biological membranes [42]. It is a highly destructive process in cellular organelles and whole organism. The loss of biochemical function and/or structural architecture may lead to damage or death of cells. Depletion of glutation results in enhanced lipid peroxidation [43]. It is evident from our results that 18-month-old rats have more lipid peroxidation, lower GSH levels, and less SOD, CAT, and GPx activity in comparison to young ones. Such an age-induced augmentation in the level of lipid peroxidation was significantly ameliorated by regular administration of melatonin and CAPE. In addition, the level of MDA was significantly lower in the experimental groups ($p < .05$ vs. group 1) compared to those of the young rats. Moreover, GSH levels and SOD activities were higher in CAPE and melatonin administered rats than that of young rats. The reduction in MDA content and the elevation in GSH levels and SOD, CAT, and GPx activities in CAPE and melatonin-treated animals suggest that these agents may scavenge the free radicals formed during aging-induced oxidative stress. Melatonin is known to be a multifaceted free radical scavenger and antioxidant [44]. It crosses all morphophysiological barriers and distributes throughout the cell [45]. We have recently reported that melatonin protects liver from age-related oxidative damage by decreasing tissue MDA level but increasing tissue GSH level and GSH-Px activity in rats. We observed that both melatonin and CAPE are effective in protecting hepatocyte ultrastructure during aging [46]. On the other hand, CAPE treatment was reported to protect the kidney from ischemia–reperfusion injury [47] and diabetic renal oxidative damage [48]. CAPE and melatonin are potent antioxidants and have high cellular protective effects.

In summary, this study shows that the glomerular and tubular structures are altered in aging. Supplemental administration of both CAPE and melatonin is beneficial in delaying age-related cellular changes. To our knowledge this is the first experimental study evaluating the effect of CAPE on aging-associated kidney damage.

Declaration of interest: The authors report no conflicts of interest. The authors alone are responsible for the content and writing of the paper.

REFERENCES

1. Pérez VI, Bokov A, Van Remmen H, et al. Is the oxidative stress theory of aging dead? *Biochim Biophys Acta*. 2009; 1790: 1005–1014.
2. Radke J. Renal physiology series, part 6 of 8: the aging kidney: structure, function, and nursing practice implications. *ANNA J*. 1994; 21: 181–190 quiz 191–193.
3. Mühlberg W, Platt D. Age-dependent changes of the kidneys: pharmacological implications. *Gerontology*.1999; 45: 243–253.
4. Lindeman RD, Goldman R. Anatomic and physiologic age changes in the kidney. *Exp Gerentol*. 1986; 21: 379–406.

5. Reiter RJ. Pineal function during aging: attenuation of the melatonin rhythm and its neurobiological consequences. *Acta Neurobiol Exp (Wars)*1994; 54: 13–19.
6. Reiter RJ. Oxygen radical detoxification process during aging: the functional importance of melatonin.*Aging (Milano)*1995; 7: 340–351.
7. Ogeturk M, Kus I, Colakoglu N, Zararsiz I, Ilhan N, Sarsilmaz M. Caffeic acid phenethyl ester protects kidneys against carbon tetrachloride toxicity in rats. *J Ethnopharmacol.* 2005; 97: 273–280.
8. Ocak S, Gorur S, Hakverdi S, Celik S, Erdogan S. Protective effects of caffeic acid phenethyl ester, vitamin C, vitamin E and *N*-acetylcysteine on vancomycin-induced nephrotoxicity in rats. *Basic Clin Pharmacol Toxicol.* 2007; 100: 328–233.
9. Ozguner F, Armagan A, Koyu A, Caliskan S, Koylu H. A novel antioxidant agent caffeic acid phenethyl ester prevents shock wave-induced renal tubular oxidative stress. *Urol Res.* 2005; 3: 239–243.
10. Grunberger D, Banerjee R, Eisinger K, et al. Preferential cytotoxicity on tumour cells by caffeic acid phenetyl ester isolated from propolis. *Experientia.* 1988; 44: 230–232.
11. Luck H. *Methods of Enzymatic Analysis.* New York: Academic Press; 1963.
12. McCord JM, Fridovich I. Superoxide dismutase: an enzymatic function for erythrocuprein (hemocuprein). *J Biol Chem.* 1969; 244: 6049–6055.
13. Lawrence RA, Burk RF. Glutathione peroxidase activity in selenium-deficient rat liver. *Biochem Biophys Res Commun*. 1976; 71: 952–958.
14. Theodorus P, Akerboom M, Sies H. Assay of glutathione, glutathione disulfide and glutathione mixed disulfides in biological samples. *Methods Enzymol*. 1981; 77: 373–383.
15. Buege AJ, Aust SD. Microsomal lipid peroxidation. *Methods Enzymol.* 1978; 52: 302–310.
16. Bradford MM. A rapid and sensitive method for the quantitation of microgram quantities of protein utilizing the principle of protein-dye binding. *Anal Biochem.* 1976; 72: 248–254.
17. Kaplan C, Pasternack B, Shah H, Gallo G. Age-related incidence of sclerotic glomeruli in human kidneys.*Am J Pathol*. 1975; 80: 227–234.
18. Neugarten J, Gallo G, Sibiger S, Kasiske B. Glomerulosclerosis in aging humans is not influenced by gender.*Am J Kidney Dis*. 1999; 34: 884–888.
19. Brenner BM. Hemodynamically mediated glomerular injury and the progressive nature of kidney disease.*Kidney Int*. 1983; 23: 647–655.
20. Anderson S, Brenner BM. Effects of aging on the renal glomerulus. *Am J Med*. 1986; 80: 435–442.
21. Langeveld JP, Veerkamp JH, Duyf CM, Monnens LH. Chemical characterization of glomerular and tubular basement membrane of men of different age. *Kidney Int.* 1981; 20: 104–114.
22. Karttunen T, Risteli J, Autio-Harmainen H, Risteli L. Effect of age and diabetes on type IV collagen and laminin in human kidney cortex. *Kidney Int*. 1986; 30: 586–591.
23. Dontas AS, Merketos SG, Papanayioutou P. Mechanisms of renal tubular defects in old age. *J Postgrad Med.* 1972; 48: 295–303.
24. Inserra F, Basso N, Ferder M, et al. Changes seen in the aging kidney and the effect of blocking the renin-angiotensin system. *Ther Adv Cardiovasc Dis.* 2009; 3: 341–346.
25. Nakano M, Ito Y, Kohtani K, Mizuno T, Tauchi H. Age-related change in brush borders of rat kidney cortex. *Mech Ageing Dev*. 1985; 33: 95–102.
26. Sato T, Tauchi H. Age changes of mitochondria of rat kidney. *Mech Ageing Dev.* 1982; 20: 111–126.
27. Ikeda H, Tauchi H, Sato T. Fine structure analysis of lipofuscin in various tissues of rats of different ages. *Mech Ageing Dev*. 1985; 33: 77–93.
28. Singh NP, Ogburn CE, Wolf NS, vanBelle G, Martin GM. DNA double-strand breaks in mouse kidney cells with age.*Biogerontology.* 2001; 2: 261–270.
29. Kujoth GC, Hiona A, Pugh TD, et al. Mitochondrial DNA mutations, oxidative stress, and apoptosis in mammalian aging. *Science.* 2005; 309: 481–484.
30. Herbert B, Pitts AE, Baker SI, et al. Inhibition of human telomerase in immortal human cells leads to progressive telomer shortening and cell death. *Proc Natl Acad Sci USA.*1999; 96: 14276–14281.
31. Melk A, Ramassar V, Helms LM, et al. Telomere shortening in kidneys with age.*J Am Soc Nephrol.* 2000; 11: 444–453.
32. Percy C, Pat B, Poronnik P, Gobe G.Role of oxidative stress in age-associated chronic kidney pathologies. *Adv Chronic Kidney Dis.* 2005; 12: 78–83.
33. Esrefoglu M, Gul M, Seyhan M, Parlakpinar H. Ultrastructural clues for potent therapeutic effect of melatonin on aging skin in pinealectomized rats. *Fundam Clin Pharmacol.* 2006; 20: 605–611.
34. Esrefoglu M, Gul M, Ates B, Yilmaz I. The ultrastructural and biochemical evidences of the beneficial effects of chronic caffeic acid phenethyl ester and melatonin administration on brain and cerebellum of aged rats. *Fundam Clin Pharmacol.* 2010; 24: 305–315.
35. Boveris A, Costa L, Cadenas E. The mitochondrial production of oxygen radicals and cellular aging.In: Cadenas E, Packer L *Understanding the Process of Aging*. New York: Dekker; 1999: 1–16.
36. de Cavanagh EM, Piotrkowski B, Basso N, et al. Enalapril and losartan attenuate mitochondrial dysfunction in aged rats. *FASEB J*. 2003; 17: 1096–1098.
37. Esrefoglu M, Gul M, Ates B, Erdogan A. The effecs of caffeic acid and phenethyl ester and melatonin on age-related vascular remodeling and cardiac damage. *Fundam Clin Pharmacol*. 2011; 25: 580–590.
38. Cakatay U, Aydin S, Yanar K, Uzun H. Gender-dependent variations in systemic biomarkers of oxidative protein, DNA, and lipid damage in aged rats. *Aging Male.* 2010; 13: 51–58
39. Rotruck JT, Pope AL, Ganther HE, Swanson AB, Hafeman DG, Hoextra WG. Selenium: biochemical role as a component of glutathione peroxidase. *Science*. 1973; 179: 588–590.
40. Liu A, Ma Y, Zhu Z. Protective effect of selenoarginine against oxidative stress in d-galactose-induced aging mice. *Biosci Biotech Biochem.* 2009; 73: 1461–1464.
41. Cui X, Zuo P, Zhang Q, et al. Chronic system d-galactose exposure induces memory loss, neurodegeneration, and oxidative damage in mice: protective effects of R-alpha-lipoic acid. *J Neurosci Res*. 2006; 84: 647–654.
42. Leyko W, Bartosz G. Membrane effects of ionizing radiation and hyperthermia. *Int J Radiat Biol Relat Stud Phys Chem Med.* 1986; 49: 734–770.
43. Comporti M. Glutathione depleting agents and lipid peroxidation. *Chem Phys Lipids*. 1987; 45: 143–169.
44. Tan DX, Manchester LC, Reiter RJ, Qi WB,Karbownik M, Calvo JR. Significance of melatonin in antioxidative defense system: reactions and products. *Biol Signals Recept.* 2000; 137–159.
45. Reiter RJ. Functional pleiotropy of the neurohormone melatonin: antioxidant protection and neuroendocrin regulation.*Front Neuroendocrinol*. 1995; 16: 383–415.
46. Esrefoglu M, Iraz M, Ates B, Gul M. Melatonin and CAPE are able to prevent the liver from oxidative damage in rats: an ultrastructural and biochemical study. *Ultrastructr Pathol*. In press.
47. Gurel A, Armutcu F, Sahin S,et al. Protective role of alpha-tocopherol and caffeic acif phenethyl ester on ischemia–reperfusion injury via nitric oxide and myeloperoxidase in rat kidneys. *Clin Chim Acta*. 2004; 339: 33–41.
48. Yilmaz HR, Uz E, Yucel N, Altuntas I, Ozcelik N. Protective effect of caffeic acid phenethyl ester (CAPE) on lipid peroxidation and antioxidant enzymes in diabetic rat liver. *J Biochem Mol Toxicol*. 2004; 18: 234–238.